GEOLOGY | THE GEOLOGICAL SOCIETY OF AMERICA®

https://doi.org/10.1130/G55209.1

Manuscript received 12 January 2026
Revised manuscript received 28 July 2026
Manuscript accepted 5 August 2026

Published online 21 August 2026

The world's highest late Middle-Pleistocene marine deposits on the southern margin of the Central Anatolian Plateau (southern Türkiye)

Selma Sarı[1,*], Paola Cipollari[1], Costanza Faranda[1], Nazik Öğretmen[2,3], Massimo Mattei[1], Francesca Cifelli[1], Irene Cornacchia[4], Fabrizio Lirer[5], Süheyla Kanbur[6], Simone Racano[1], Elsa Gliozzi[1], and Domenico Cosentino[1]
[1]Department of Sciences, Roma Tre University, 00154 Rome, Italy
[2]Algarve Centre of Marine Sciences, University of Algarve, 8005-139 Faro, Portugal
[3]Portuguese Institute for Sea and Atmosphere, 1495-165 Algés, Portugal
[4]Institute of Environmental Geology and Geoengineering of the National Research Council, 00015 Montelibretti, Italy
[5]Department of Earth Sciences, Sapienza University of Rome, 00185 Rome, Italy
[6]Department of Geological Engineering, Süleyman Demirel University, 32260 Isparta, Turkey

ABSTRACT

Reconstructing surface uplift rates in active orogens is critical for understanding how deep Earth processes shape topography, but such estimates require both rapid uplift and preservation of young marine deposits. The southern margin of the Central Anatolian Plateau (CAP) in Türkiye provides an exceptional example, preserving Upper Miocene and late Middle-Pleistocene marine deposits at ∼2.2 km and ∼1.1 km of elevation, respectively, indicating multiphase uplift. We investigated the TOL-1 section in the Mut Basin, which preserves late Middle-Pleistocene (Marine Isotope Stage 7) marine deposits at 1177 m above mean sea level (amsl); the highest in the world. The section records two key calcareous nannofossil bioevents: the last occurrence of *Pseudoemiliania lacunosa* (0.46 Ma) and the first occurrence of *Emiliania huxleyi* (0.26 Ma). Foraminiferal biostratigraphy, marked by the consistent presence of *Globigerinella calida* from the base, indicates that deposition began after ca. 0.53 Ma. Ostracod assemblages reveal a transition from upper epibathyal to littoral environments, with a shallowing-upward trend beginning at ca. 0.40 Ma. Paleomagnetic data indicate normal polarity, consistent with deposition during the current normal polarity Brunhes Chron. By integrating biostratigraphy, paleobathymetric reconstructions (∼50 m below mean sea level), and sea-level estimates at 0.23 Ma (∼−18 m), we calculated a mean uplift rate of ∼5.2 m/k.y. This exceptionally high rate may be attributed to slab break-off of the still-subducting eastern Cyprus slab combined with mantle flow from the Arabian slab window at the Eastern Anatolian collision zone. These findings provide a rare high-resolution temporal benchmark for linking stratigraphic records of marine deposition with deep-seated processes and rapid surface uplift in active convergent margins.

INTRODUCTION

Orogenic plateaus such as Tibet, the Altiplano-Puna (South America), and Anatolia (Türkiye) provide natural laboratories for investigating how deep Earth processes shape surface evolution (e.g., Garzione et al., 2017; Göğüş et al., 2017; Zhang et al., 2021). Situated within the Africa–Eurasia convergence zone, the Central Anatolian Plateau (CAP) exemplifies a tectonic setting where uplift reflects complex mantle-driven processes, including slab segmentation, break-off, lithospheric dripping, continental underthrusting of the African margin, and delamination by peeling (Cosentino et al., 2012; Schildgen et al., 2012, 2014; McPhee et al., 2022; Aykut et al., 2025).

The CAP interior is a low-relief surface surrounded by high-relief margins, most prominently the Central Taurides to the south. In this fold-and-thrust belt, post-thrusting extension followed by marine sedimentation (preserved in the Antalya, Mut, and Adana basins) records multiple phases of uplift (Cosentino et al., 2012; Schildgen et al., 2012, 2014; Öğretmen et al., 2018). Notably, marine sedimentation persisted in several sub-basins, and recent micropaleontological studies demonstrate that the youngest marine units in the Aksu (Kanbur and Öğretmen, 2022), Manavgat (Sarı et al., 2026), and Mut (Yıldız et al., 2003) basins extend into the Quaternary (Fig. 1A).

In the Mut Basin (Fig. 1B), high-elevation marine deposits have been recently reinterpreted as Lower to Middle Pleistocene (Öğretmen et al., 2018). Those authors established the Gülnar East section (983 m above mean sea level [amsl]) as Lower Pleistocene (from 1.73 Ma to 1.10 Ma), and the TOL section (1087 m amsl) as Middle Pleistocene (from ca. 0.61 Ma to ca. 0.46 Ma), implying mean uplift rates of 3.2–3.4 m/k.y. These findings highlight rapid Quaternary surface uplift of the CAP southern margin, which continues today at rates of 0.9–1.5 m/k.y. as constrained by late Holocene sea-level markers (Liberatore et al., 2022).

We present new biostratigraphic, paleomagnetic, and paleobathymetric data from the TOL-1 section, located ∼0.4 km from the TOL section of Öğretmen et al. (2018), at 1177 m of elevation (Fig. 1B). The section records marine deposition until ca. 0.23 Ma, demonstrating that marine conditions along the southern CAP margin persisted longer than previously recognized. We aim to (1) refine the timing and magnitude of the Middle Pleistocene uplift

Selma Sarı https://orcid.org/0000-0003-0963-3325
*ssari@os.uniroma3.it

CITATION: Sarı, S., et al., 2026, The world's highest late Middle-Pleistocene marine deposits on the southern margin of the Central Anatolian Plateau (southern Türkiye): Geology, v. XX, p. , https://doi.org/10.1130/G55209.1

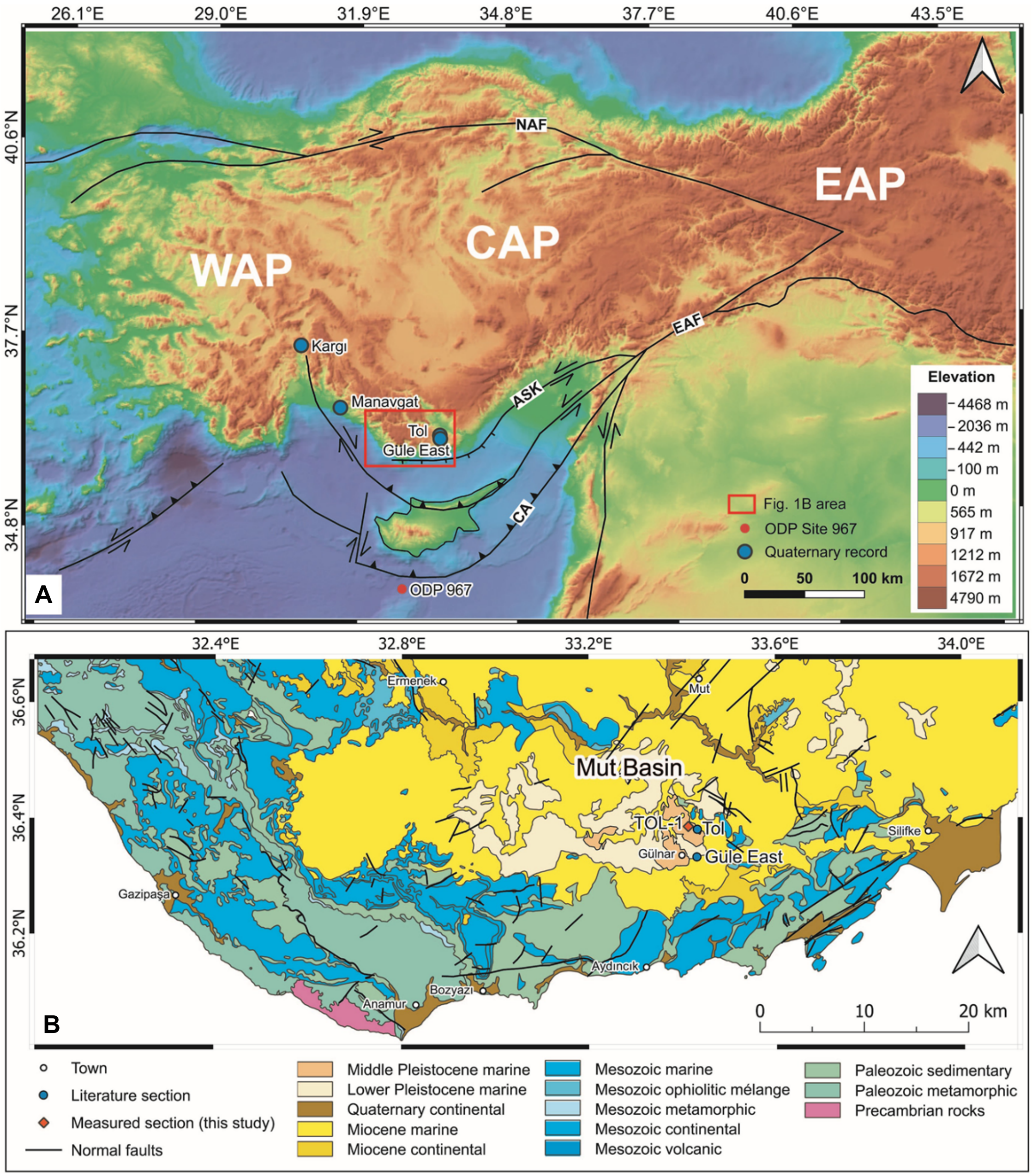

Figure 1. (A) Simplified regional tectonic map of Anatolia (Türkiye) showing the locations of Quaternary marine records and Ocean Drilling Program (ODP) Site 967. CAP—Central Anatolian Plateau; EAP—Eastern Anatolian Plateau; WAP—Western Anatolian Province; NAF—North Anatolian fault; EAF—East Anatolian fault; CA—Cyprus arc; ASK—Anamur-Silifke-Kozan fault. (B) Geological map of the southern margin of the CAP showing the location of the TOL-1 section (modified after Racano et al., 2021).

along the CAP southern margin, (2) place the CAP's Middle Pleistocene marine record into a global framework by comparing it with coeval stratigraphic sections from other tectonic settings, and (3) hypothesize possible geodynamic processes responsible for this rapid surface response.

METHODS

The TOL-1 section (36.385225°N, 33.424114°E; 1177 m amsl) is in the Mut Basin of southwestern Türkiye (Fig. 1B). This ~71-m-thick succession comprises a shallowing-upward marine sequence of marls, clayey marls, and interbedded calcarenites (Fig. 2). We collected 68 bulk samples for micropaleontological, geochemical, and paleomagnetic analyses. We quantitatively analyzed calcareous nannofossils using smear slides on a per-unit-area basis (Backman and Shackleton, 1983). To improve the detection of the coccolithophore *Emiliania huxleyi*, the uppermost 23 samples (labeled TOL-1A 1–23) were processed using the concentration techniques of de Capoa et al. (2003). Results were classified according to the biostratigraphic scheme of Di Stefano et al. (2023). We qualitatively studied planktonic foraminifers to support biostratigraphic dating, following the biostratigraphic zonation of Lirer et al. (2019). Ostracod assemblages were analyzed quantitatively using Bray–Curtis similarity cluster analysis and the unweighted pair-group method with arithmetic mean to constrain paleobathymetry. We performed oxygen stable-isotope analyses ($\delta^{18}O$) on planktonic foraminifer *Trilobatus trilobus*. We picked between 10 and 15 specimens of *T. trilobus* from 30 samples and performed the analyses using a Thermo Delta V Advantage mass spectrometer at the Geochemical Laboratory of the Earth Science Department of Sapienza University (Rome, Italy). Calibration to Vienna Peedee belemnite (VPDB) was carried out following NBS-19 limestone standards (Coplen et al., 1996). We compared the results with reference formanifer *Globigerinoides ruber* $\delta^{18}O$ data from Ocean Drilling Program (ODP) Site 967 (Grant et al., 2022). We collected a total of 67 oriented samples for magnetostratigraphy. Alternating field demagnetization (up to 100 mT) was performed with a 2G SQUID cryogenic magnetometer at the National Institute of Geophysics and Volcanology (INGV; Rome, Italy) to isolate the characteristic remanent magnetization (Butler, 1992).

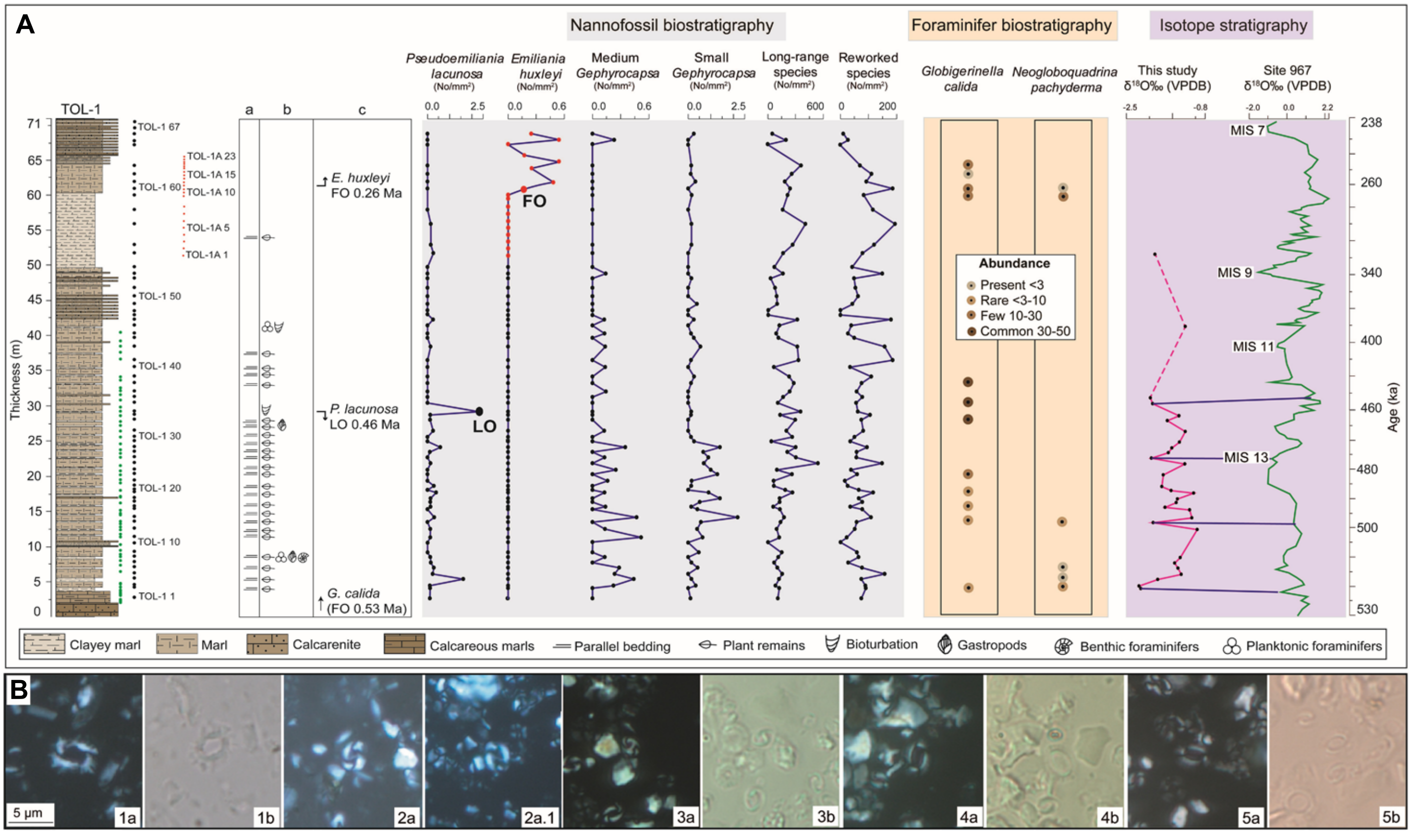

Figure 2. (A) Stratigraphy of the TOL-1 section in Türkiye (location shown in Fig. 1) showing the abundance of selected calcareous nannofossil and planktonic foraminiferal marker taxa and the δ¹⁸O record from *Trilobatus trilobus* compared with δ¹⁸O from *Globigerinoides ruber* of Ocean Drilling Program (ODP) Site 967 (Grant et al., 2022). Green dots indicate sampling locations for the paleomagnetic analyses, black dots represent the samples collected for the micropaleontological analyses, and red dots indicate the samples processed using the concentration technique to detect *Emiliania huxleyi*. Purple horizontal lines indicate correlations between interglacial peaks; δ¹⁸O age tie-points are shown on the right. a—sedimentary structures; b— fossil components; c—biostratigraphic events; LO—last occurrence; FO—first occurrence; VPDB—Vienna Peedee belemnite; MIS—marine isotope stage. (B) Microphotographs of calcareous nannofossils of the TOL-1 section. (1a, 1b) *Pseudoemiliania lacunosa* (TOL-1 6). (2a, 2a.1) Medium *Gephyrocapsa* (TOL-1 21, TOL-1 28). (3a, 3b) Small *Gephyrocapsa* (TOL-1A 12). (4a, 4b, 5a, 5b) *Emiliania huxleyi* (TOL-1 65, TOL-1A 21). "a" indicates crossed nicols; "b" indicates parallel nicols. Scale bar is uniform across all images.

RESULTS

Calcareous nannofossil assemblages are dominated by long-range and reworked taxa, whereas marker species (*E. huxleyi, Gephyrocapsa* spp., and *Pseudoemiliania lacunosa*) are scarce (Fig. 2A). Long-range forms occur consistently, while reworked taxa comprise ~30% on average, locally reaching ~60% of the total assemblage (Figs. S1 and S2 in the Supplemental Material[1]). *Gephyrocapsa* spp. and *E. huxleyi* rarely exceed 1%–2%. Two bioevents were recognized: the last occurrence (LO) of *P. lacunosa* (0.46 Ma), and the first occurrence (FO) of *E. huxleyi* (0.26 Ma). Isolated *P. lacunosa* specimens above its LO are interpreted as reworked.

The planktonic foraminifers in the TOL-1 section are generally poorly to moderately preserved and moderately diversified, resulting in several indeterminate specimens. The assemblage includes *Globigerinodes quadrilobatus, Globigerinodes obliquus obliquus, Trilobatus trilobus, Globigerinella calida, Globoturborotalita rubescens, Globigerinita glutinata, Neogloboquadrina pachyderma, N. incompta, N. dutertrei, Globigerinoides ruber* (white), *Globigerinoides tenellus, Orbulina universa* and *Globigerina bulloides* (Table S1; Fig. S3). *Globigerinella calida* consistently occurs from the base of the section, constraining ages younger than ca. 0.53 Ma (FO of *G. calida*; Fig. 2A). Although this age would typically coincide with the common presence of *Globorotalia truncatulinoides* and frequent *N. pachyderma*, *G. truncatulinoides* is not observed and *N. pachyderma* occurs only sporadically in the studied section.

We detected 36 reworked and 49 autochthonous ostracod species (Tables S2 and S3). The latter are included in three different paleoecological groups: littoral, epibathyal/bathyal, and eurybathic species. The paleoenvironmental analysis of ostracods (Fig. 3; Table S3; Fig. S5) indicates that the deposition of the TOL-1 section started in a littoral (dominance of the species *Aurila convexa*), vegetated environment that deepened along the section down to the upper epibathyal environment (co-dominance of the epibathyal species *Bythocypris producta*, *Cytherella robusta,* and *Henryhowella sarsi profunda*), and became shallow littoral again (at ~50 m of depth for the presence of *Hemicytherura defiorei*) at the top of the section.

Planktonic foraminiferal δ¹⁸O of TOL-1 ranges from −2.23‰ to −0.96‰ (Fig. 2A; Table S4).

Based on our biostratigraphic age constraints, we determined different sedimentation rates: >0.41 m/k.y. at the base, 0.16 m/k.y. between the LO of *P. lacunosa* and FO of *E. huxleyi*, and ~0.45 m/k.y. in the uppermost ~5 m (Fig. S6). Consequently, the top of the TOL-1 section is dated at ca. 0.23 Ma (Fig. S6).

Forty-seven (47) of the 51 isolated characteristic remanent magnetization (ChRM) directions point down to the north, indicating normal mag-

[1]Supplemental Material. Supplemental figures and tables include calcareous nannofossil, foraminiferal, and ostracod distribution data, oxygen isotope (δ¹⁸O) measurements, paleomagnetic analyses, and a compilation of the elevation and ages of MIS 7 marine deposits worldwide used for comparison in this study. Please visit https://doi.org/10.1130/GEOL.S.33170276 to access the supplemental material; contact editing@geosociety.org with any questions.

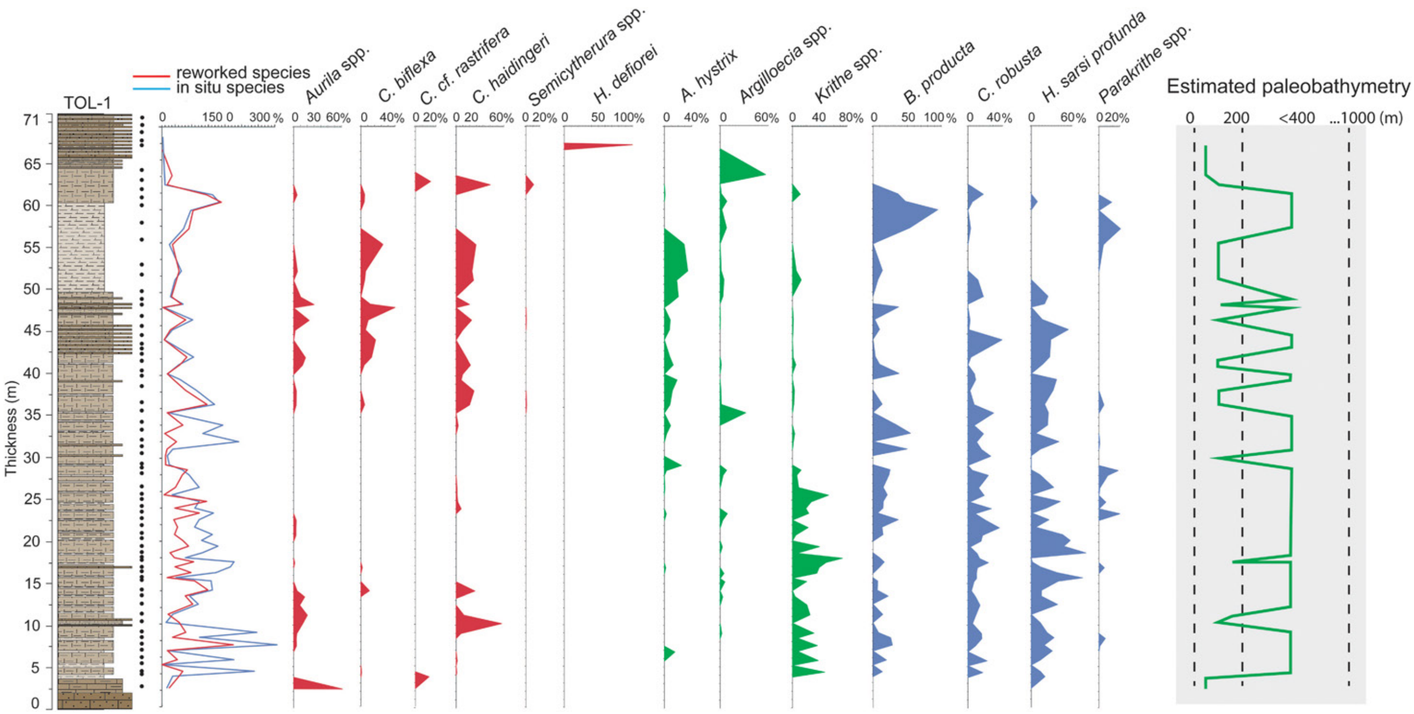

Figure 3. Ostracod assemblages and paleobathymetric reconstruction of the TOL-1 section in Türkiye (location shown in Fig. 1). Left: Percentage of autochthonous versus reworked ostracods. Center: Percentage distribution of littoral (in red), eurybathic (in green), and epibathyal (in blue) taxa. Right: Reconstructed paleobathymetric curve based on ostracod assemblages.

netic polarity consistent with deposition during the current normal polarity Brunhes Chron (Fig. S7). The remaining ChRM directions, from the lower part of the section, point down to the south and may record short-lived geomagnetic excursions. Because the top of the section (1177 m amsl) was deposited at ~50 m below msl, as inferred from ostracod assemblages, and given a late Middle-Pleistocene sea-level position at ~18 m below the present mean sea level (Antonioli et al., 2021), we calculated a mean uplift rate of ~5.2 m/k.y.

DISCUSSION

Biostratigraphic and Paleoenvironmental Signals

Despite the evident reworking, we identified two robust calcareous nannofossil bioevents that fix the age of the TOL-1 marine succession. Importantly, the FO of *E. huxleyi* (Fig. 2) near the top of TOL-1 allows us to extend the marine conditions in the Mut Basin up to ca. 0.23 Ma.

Planktonic foraminifers provide independent support for the Middle Pleistocene age for the TOL-1 section. The presence of *Globigerinella calida* from the base of the section indicates marine deposition began after 0.53 Ma (Fig. S3). Notably, color variant *Globigerinoides ruber* pink was not observed in the section, although it is commonly reported during interglacial periods elsewhere in the Mediterranean (e.g., Marine Isotope Stage [MIS] 11 in the east, MIS 9 in the west, and Holocene/MIS 5e in the west; Pérez-Folgado et al., 2004; Numberger et al., 2009). A proposed FO at ca. 0.33 Ma in the eastern Mediterranean (Lirer et al., 2019) remains uncertain due to the lack of published supporting evidence. Its sporadic distribution suggests ecological factors may influence its occurrence.

Based on the calcareous plankton bioevents, we propose a possible correlation between the $\delta^{18}O$ *T. trilobus* of the TOL-1 section with the $\delta^{18}O$ *G. ruber* of ODP Site 967. This correlation allows us to constrain the study section to between MIS 14 and MIS 7 (Fig. 2A).

Ostracod assemblages show a progressive shallowing from ~400 m to ~50 m water depth, consistent with uplift-related environmental changes initiating at ca. 0.40 Ma (Fig. 3; Fig. S2). This trend is consistent with regional geomorphological and geochronological evidence for accelerated uplift and river incision beginning at ca. 0.45 Ma (Racano et al., 2020, 2021; Aykut et al., 2025), while increased reworking of calcareous nannofossils of the TOL-1 section further supports enhanced uplift and/or erosion during this interval (Fig. S2).

Implications for the Uplift History of the CAP Southern Margin

The southern margin of the CAP records a multiphase uplift history, preserving Upper Miocene and Middle Pleistocene marine sediments at ~2.2 km and ~1 km of elevation, respectively (Schildgen et al., 2012; Öğretmen et al., 2018). The youngest previously dated marine sediments (ca. 0.45 Ma), deposited at paleodepths of ~400–500 m and now exposed at ~1 km elevation, imply uplift rates of ~3.2–3.4 m/k.y., peaking between ca. 0.5 Ma and 0.2 Ma (Öğretmen et al., 2018; Racano et al., 2020). Our age model from TOL-1 demonstrates that marine conditions persisted until at least ca. 0.23 Ma, and indicates even higher uplift rates of ~5.2 m/k.y., suggesting more intense and rapid uplift than previously recognized.

Previous studies linked uplift of the southern CAP to slab break-off beneath the Cyprus subduction zone and associated mantle upwelling (Cosentino et al., 2012; Schildgen et al., 2012, 2014; Duretz and Gerya, 2013), whereas McPhee et al. (2022) additionally proposed underthrusting of the African continental margin beneath southern Anatolia at ca. 0.45 Ma based on the youngest marine deposits identified by Öğretmen et al. (2018).

However, the partitioning of vertical motions within the Cyprus subduction system allows us to rule out any contribution of the underthrusting process to the late Middle-Pleistocene uplift of the CAP southern margin. Above the underthrusting zone of the Cyprus subduction system (Fig. 4), MIS 7 deposits occur at 8–11 m amsl (south of the Kyrenia thrust) and 40 m amsl (north of the Kyrenia thrust) (Palamakumbura et al., 2016), in contrast to the 1177 m elevation of TOL-1, ~230 km farther from the Cyprus trench. This different elevation was likely accommodated by the still-active Anamur-Silifke-Kozan (ASK) fault system (Ozel et al., 2007), which mechanically decoupled the Cyprus arc from the CAP southern margin.

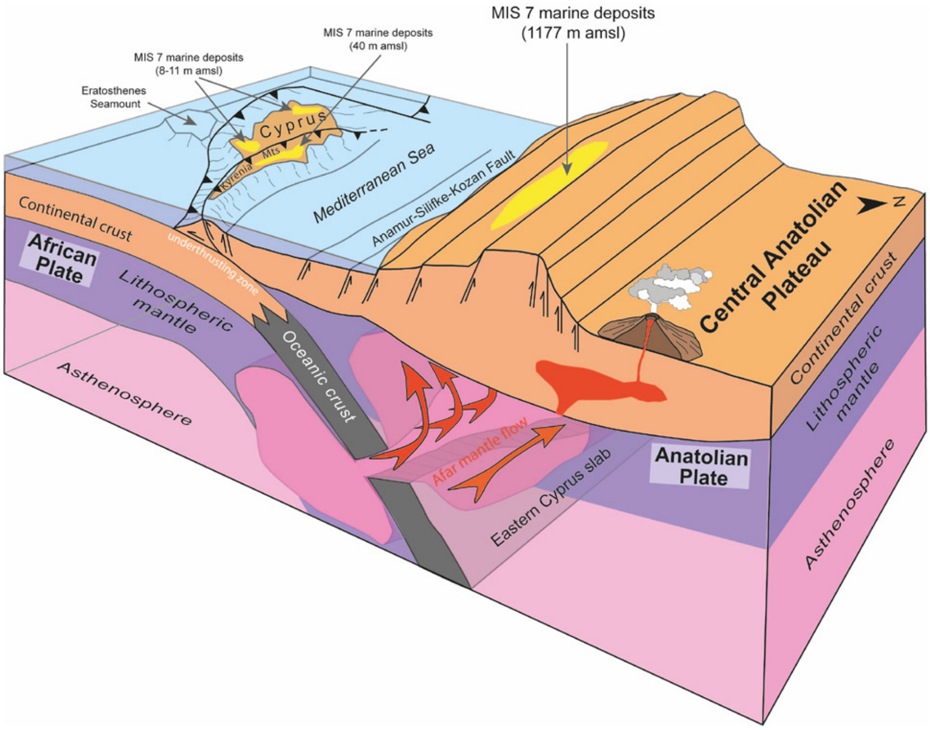

Figure 4. Cartoon illustrating the uplift of the world's highest late Middle-Pleistocene marine deposits (Marine Isotope Stage [MIS] 7) at the CAP southern margin as a consequence of multiple interacting mantle flow systems (see text for additional explanations). amsl—above mean sea level.

Globally, late Middle-Pleistocene (MIS 7) marine deposits are generally preserved at relatively low elevations (<60 m on passive margins, and commonly <300 m even in tectonically active settings), making TOL-1 deposits at 1177 m exceptional outliers (Table S5; Fig. S8). The uniqueness of the uplift of MIS 7 from the TOL-1 section within a global context is likely related to the complex geodynamic setting of the colliding Anatolian, Arabian, and African plates, which exhibits multiple interacting mantle flow systems (e.g., Faccenna et al., 2014; Confal et al., 2018). In this scenario, the return flow of the Hellenic slab beneath Anatolia (Faccenna et al., 2014), combined with the northward-directed mantle flow from the Arabian slab break-off at the Eastern Anatolian collision zone (Afar mantle flow; Faccenna et al., 2013) and the asthenosphere upwelling through the eastern Cyprian slab window (e.g., Biryol et al., 2011; Portner et al., 2018; Aydın et al., 2022) after the collision of the Eratosthenes Seamount with the Anatolian plate (Robertson, 1998), define one of the most complex examples of mantle circulation, which, in our opinion, is responsible for the recent strong uplift rate and volcanism at the CAP southern margin.

CONCLUSIONS

Along the southern margin of the CAP, Middle Pleistocene (post–0.53 Ma) marine sediments of the TOL-1 section occur higher than at any place on Earth (~1177 m amsl). Integration of calcareous nannofossil and planktonic foraminiferal biostratigraphy, ostracod-based paleobathymetric reconstruction, $\delta^{18}O$ stratigraphy, and paleomagnetic data indicates that marine deposition in the Mut Basin persisted until at least ca. 0.23 Ma, implying a mean surface uplift rate of ~5.2 m/k.y. along the southern CAP margin. This exceptional rate of uplift might be explained by multiple interacting upper-mantle flow systems following the opening of the eastern Cyprian slab window as a consequence of the collision of the Eratosthenes Seamount with the Anatolian plate. Our findings provide an important temporal constraint linking marine stratigraphy with deep-seated processes and rapid surface uplift in active convergent margins.

ACKNOWLEDGMENTS

We acknowledge a grant to the Department of Science, Roma Tre University (MIUR—Italy Department of Excellence, article 1, paragraph 314–337, law 232/2016). Special thanks to Patrizia Maiorano for calcareous nannofossil discussions and to Francesco Salvini for providing the ENVI software. The authors sincerely thank the editor, Rob Strachan, and the reviewers, Douwe van Hinsbergen, Clay Campbell, and an anonymous reviewer, for their thoughtful, constructive, and insightful comments. Their valuable suggestions substantially improved the quality, clarity, and scientific interpretation of this manuscript.

REFERENCES CITED

Antonioli, F., Furlani, S., Montagna, P., and Stocchi, P., 2021, The use of submerged speleothems for sea level studies in the Mediterranean Sea: A new perspective using Glacial Isostatic Adjustment (GIA): Geosciences, v. 11, https://doi.org/10.3390/geosciences11020077.

Aydın, F., Sönmez, M., Siebel, W., Karsli, O., and Lermi, A., 2022, Slab break-off-related magnesian andesites and dacites with adakitic affinity from the early Quaternary Keçiboyduran stratovolcano, Cappadocia province, central Turkey: Evidence for slab/sediment melt–mantle interaction and magma mixing: Contributions to Mineralogy and Petrology, v. 177, 65, https://doi.org/10.1007/s00410-022-01931-8.

Aykut, T., Yıldırım, C., Uysal, I.T., Ring, U., and Zhao, J.X., 2025, Coeval upper crustal extension and surface uplift in the Central Taurides (Türkiye) above the Cyprus Subduction Zone: Nature Communications, v. 16, 3921, https://doi.org/10.1038/s41467-024-55802-w.

Backman, J., and Shackleton, N.J., 1983, Quantitative biochronology of Pliocene and early Pleistocene calcareous nannofossils from the Atlantic, Indian and Pacific oceans: Marine Micropaleontology, v. 8, p. 141–170, https://doi.org/10.1016/0377-8398(83)90009-9.

Biryol, B.C., Beck, S.L., Zandt, G., and Özacar, A.A., 2011, Segmented African lithosphere beneath the Anatolian region inferred from teleseismic P-wave tomography: Geophysical Journal International, v. 184, p. 1037–1057, https://doi.org/10.1111/j.1365-246X.2010.04910.x.

Butler, R.F., 1992, Paleomagnetism: Magnetic Domains to Geologic Terrains: Boston, Blackwell Scientific Publications, 319 p.

Confal, J.M., Faccenda, M., Eken, T., and Taymaz, T., 2018, Numerical simulation of 3-D mantle flow evolution in subduction zone environments in relation to seismic anisotropy beneath the eastern Mediterranean region: Earth and Planetary Science Letters, v. 497, p. 50–61, https://doi.org/10.1016/j.epsl.2018.06.005.

Coplen, T.B., De Bièvre, P., Krouse, H.R., Vocke, R.D., Jr., Gröning, M., and Rozanski, K., 1996, Ratios for light-element isotopes standardized for better interlaboratory comparison: Eos (Transactions, American Geophysical Union), v. 77, p. 255, https://doi.org/10.1029/96EO00182.

Cosentino, D., Schildgen, T.F., Cipollari, P., Faranda, C., Gliozzi, E., Hudáčková, N., and Strecker, M.R., 2012, Late Miocene surface uplift of the southern margin of the Central Anatolian Plateau, Central Taurides, Turkey: Geological Society of America Bulletin, v. 124, p. 133–145, https://doi.org/10.1130/B30466.1.

De Capoa, P., Di Donato, V., Di Staso, A., Giardino, S., and Rinaldi, S., 2003, Preparation techniques and methodological approach to calcareous nannofossil analysis in silico- and calciclastic turbidites: Courier Forschungsinstitut Senckenberg, v. 244, p. 105–127.

Di Stefano, A., Baldassini, N., Raffi, I., Fornaciari, E., Incarbona, A., Negri, A., Bonomo, S., Villa, G., Di Stefano, E., and Rio, D., 2023, Neogene-Quaternary Mediterranean calcareous nannofossil biozonation and biochronology: A review: Stratigraphy, v. 20, p. 259, https://doi.org/10.29041/strat.20.4.02.

Duretz, T., and Gerya, T.V., 2013, Slab detachment during continental collision: Influence of crustal rheology and interaction with lithospheric delamination: Tectonophysics, v. 602, p. 124–140, https://doi.org/10.1016/j.tecto.2012.12.024.

Faccenna, C., Becker, T.W., Jolivet, L., and Keskin, M., 2013, Mantle convection in the Middle East: Reconciling Afar upwelling, Arabia indentation and Aegean trench rollback: Earth and Planetary

Science Letters, v. 375, p. 254–269, https://doi.org/10.1016/j.epsl.2013.05.043.
Faccenna, C., et al., 2014, Mantle dynamics in the Mediterranean: Reviews of Geophysics, v. 52, p. 283–332, https://doi.org/10.1002/2013RG000444.
Garzione, C.N., et al., 2017, Tectonic evolution of the Central Andean plateau and implications for the growth of plateaus: Annual Review of Earth and Planetary Sciences, v. 45, p. 529–559, https://doi.org/10.1146/annurev-earth-063016-020612.
Göğüş, O.H., Pysklywec, R.N., Şengör, A.M.C., and Gün, E., 2017, Drip tectonics and the enigmatic uplift of the Central Anatolian Plateau: Nature Communications, v. 8, 1538, https://doi.org/10.1038/s41467-017-01611-3.
Grant, K.M., et al., 2022, Organic carbon burial in Mediterranean sapropels intensified during Green Sahara Periods since 3.2 Myr ago: Communications Earth & Environment, v. 3, 11, https://doi.org/10.1038/s43247-021-00339-9; correction available at https://doi.org/10.1038/s43247-022-00357-1.
Kanbur, S., and Öğretmen, N., 2022, Revised late Cenozoic foraminifer biostratigraphy of the Eskiköy Formation (Aksu Basin), SW Turkey and its paleoenvironmental conditions: Palaeogeography, Palaeoclimatology, Palaeoecology, v. 591, https://doi.org/10.1016/j.palaeo.2022.110883.
Liberatore, M., Gliozzi, E., Cipollari, P., Öğretmen, N., Spada, G., and Cosentino, D., 2022, Vertical velocity fields along the Eastern Mediterranean coast as revealed by late Holocene sea-level markers: Earth-Science Reviews, v. 234, https://doi.org/10.1016/j.earscirev.2022.104199.
Lirer, F., Foresi, L.M., Iaccarino, S.M., Salvatorini, G., Turco, E., Cosentino, C., Sierro, F.J., and Caruso, A., 2019, Mediterranean Neogene planktonic foraminifer biozonation and biochronology: Earth-Science Reviews, v. 196, https://doi.org/10.1016/j.earscirev.2019.05.013.
McPhee, P.J., van Hinsbergen, D.J.J., and Koç, A., 2022, Reply to comment on "Preparing the ground for plateau growth: Late Neogene Central Anatolian uplift in the context of orogenic and geodynamic evolution since the Cretaceous": Tectonophysics, v. 836, https://doi.org/10.1016/j.tecto.2022.229404.
Numberger, L., Hemleben, C., Hoffmann, R., Mackensen, A., Schulz, H., Wunderlich, J.M., and Kucera, M., 2009, Habitats, abundance patterns and isotopic signals of morphotypes of the planktonic foraminifer *Globigerinoides ruber* (d'Orbigny) in the eastern Mediterranean Sea since the Marine Isotopic Stage 12: Marine Micropaleontology, v. 73, p. 90–104, https://doi.org/10.1016/j.marmicro.2009.07.004.
Öğretmen, N., Cipollari, P., Frezza, V., Faranda, C., Karanika, K., Gliozzi, E., Radeff, G., and Cosentino, D., 2018, Evidence for 1.5 km of uplift of the Central Anatolian Plateau's southern margin in the last 450 kyr and implications for its multiphased uplift history: Tectonics, v. 37, p. 359–390, https://doi.org/10.1002/2017TC004805.
Ozel, E., Ulug, A., and Pekcetinoz, B., 2007, Neotectonic aspects of the northern margin of the Adana-Cilicia submarine basin, NE Mediterranean: Journal of Earth System Science, v. 116, p. 113–124, https://doi.org/10.1007/s12040-007-0011-9.
Palamakumbura, R.N., Robertson, A.H., Kinnaird, T.C., van Calsteren, P., Kroon, D., and Tait, J.A., 2016, Quantitative dating of Pleistocene deposits of the Kyrenia Range, northern Cyprus: Implications for timing, rates of uplift and driving mechanisms: Journal of the Geological Society, v. 173, p. 933–948, https://doi.org/10.1144/jgs2015-130.
Pérez-Folgado, M., Sierro, F.J., Flores, J.A., Grimalt, J.O., and Zahn, R., 2004, Paleoclimatic variations in foraminifer assemblages from the Alboran Sea (Western Mediterranean) during the last 150 ka in ODP Site 977: Marine Geology, v. 212, p. 113–131, https://doi.org/10.1016/j.margeo.2004.08.002.
Portner, D.E., Delph, J.R., Biryol, C.B., Beck, S.L., Zandt, G., Özacar, A.A., Sandvol, E., and Türkelli, N., 2018, Subduction termination through progressive slab deformation across Eastern Mediterranean subduction zones from updated P-wave tomography beneath Anatolia: Geosphere, v. 14, p. 907–925, https://doi.org/10.1130/GES01617.1.
Racano, S., Jara-Muñoz, J., Cosentino, D., and Melnick, D., 2020, Variable quaternary uplift along the southern margin of the central Anatolian plateau inferred from modeling marine terrace sequences: Tectonics, v. 39, https://doi.org/10.1029/2019TC005921.
Racano, S., Schildgen, T.F., Cosentino, D., and Miller, S.R., 2021, Temporal and spatial variations in rock uplift from river-profile inversions at the Central Anatolian Plateau southern margin: Journal of Geophysical Research: Earth Surface, v. 126, p. 1–23, https://doi.org/10.1029/2020JF006027.
Robertson, A.H.F., 1998, Tectonic significance of the Eratosthenes Seamount: A continental fragment in the process of collision with a subduction zone in the eastern Mediterranean (Ocean Drilling Program Leg 160): Tectonophysics, v. 298, p. 63–82, https://doi.org/10.1016/S0040-1951(98)00178-4.
Sarı, S., Cipollari, P., Faranda, C., Kanbur, S., Racano, S., and Cosentino, D., 2026, Tectono-sedimentary evolution and uplift of the Antalya Basin (southern Türkiye) during the late Middle Pleistocene: Insights from the Manavgat fan-delta complex: Marine Geoscience and Energy Resources, v. 192, https://doi.org/10.1016/j.marger.2026.207810.
Schildgen, T.F., Cosentino, D., Bookhagen, B., Niedermann, S., Yildirim, C., Echtler, H.A., and Strecker, M.R., 2012, Multi-phased uplift of the southern margin of the Central Anatolian Plateau, Turkey: A record of tectonic and upper mantle processes: Earth and Planetary Science Letters, v. 317–318, p. 85–95, https://doi.org/10.1016/j.epsl.2011.12.003.
Schildgen, T.F., Yildirim, C., Cosentino, D., and Strecker, M.R., 2014, Linking slab breakoff, Hellenic trench retreat, and uplift of the Central and Eastern Anatolian Plateaus: Earth-Science Reviews, v. 128, p. 147–168, https://doi.org/10.1016/j.earscirev.2013.11.006.
Yıldız, A., Toker, V., Demircan, H., and Sevim, S., 2003, Paleoenvironmental interpretation and findings of Pliocene–Pleistocene nannoplankton, planktic foraminifera, trace fossil in the Mut Basin: Yerbilimleri, v. 28, p. 123–144 [in Turkish with English abstract].
Zhang, M., et al., 2021, Linking deeply-sourced volatile emissions to plateau growth dynamics in southeastern Tibetan Plateau: Nature Communications, v. 12, 4157, https://doi.org/10.1038/s41467-021-24415-y.

Printed in the USA